



Spin and lattice structures of single-crystalline SrFe₂As₂

Jun Zhao,¹ W. Ratcliff II,² J. W. Lynn,² G. F. Chen,³ J. L. Luo,³ N. L. Wang,³ Jiangping Hu,⁴ and Pengcheng Dai^{1,5,*}

¹Department of Physics and Astronomy, The University of Tennessee, Knoxville, Tennessee 37996-1200, USA

²NIST Center for Neutron Research, National Institute of Standards and Technology, Gaithersburg, Maryland 20899-6012, USA

³Beijing National Laboratory for Condensed Matter Physics, Institute of Physics, Chinese Academy of Sciences, Beijing 100080, People's Republic of China

⁴Department of Physics, Purdue University, West Lafayette, Indiana 47907, USA

⁵Neutron Scattering Science Division, Oak Ridge National Laboratory, Oak Ridge, Tennessee 37831, USA

(Received 7 July 2008; revised manuscript received 7 September 2008; published 3 October 2008)

We use neutron scattering to study the spin and lattice structure of single-crystal SrFe₂As₂, the parent compound of the FeAs-based superconductor (Sr,K)Fe₂As₂. We find that SrFe₂As₂ exhibits an abrupt structural phase transition at 220 K, where the structure changes from tetragonal with lattice parameters $c > a = b$ to orthorhombic with $c > a > b$. At almost the same temperature, Fe spins develop a collinear antiferromagnetic structure along the orthorhombic a axis with spin direction parallel to this a axis. These results are consistent with earlier work on the RFeAsO (R =rare earth) families of materials and on BaFe₂As₂, and therefore suggest that static antiferromagnetic order is ubiquitous for the parent compounds of these FeAs-based high-transition temperature superconductors.

DOI: 10.1103/PhysRevB.78.140504

PACS number(s): 74.70.Dd, 75.25.+z, 75.30.Fv, 75.50.Ee

Understanding the structural, electronic, and magnetic properties of parent compounds of high-transition temperature (high- T_c) superconductors is an essential step in developing a microscopic theory for superconductivity. For high- T_c copper oxides, the parent compounds are antiferromagnetic (AFM) Mott insulators, where the nearest-neighbor Cu²⁺ spins in the CuO₂ plane arrange themselves antiferromagnetically.¹ In the case of the Fe-As-based high- T_c superconductors,²⁻⁸ while the Fe ions in parent compounds LaFeAsO (Refs. 9 and 10), CeFeAsO (Ref. 11), NdFeAsO (Ref. 12), and BaFe₂As₂ (Refs. 13 and 14) are found to exhibit commensurate static AFM long-range order, all previous neutron-scattering experiments on these FeAs-based materials were carried out on polycrystalline samples.⁹⁻¹⁴ The small differences in the a/b lattice constants in the low-temperature orthorhombic structure of LaFeAsO (Refs. 9 and 10), CeFeAsO (Ref. 11), and NdFeAsO (Ref. 12), combined with the small ordered moment that requires coarse resolution for the neutron magnetic powder-diffraction method, make it difficult to determine the spin direction and in most cases the AFM ordering wave vector for the collinear AFM structure.

In this paper, we report single-crystal neutron-scattering studies of the structural and magnetic phase transitions for SrFe₂As₂, the parent compound of the (Sr,K)Fe₂As₂ superconductors.^{8,15} Previous transport,⁵⁷Fe Mössbauer, and x-ray diffraction experiments¹⁶⁻¹⁸ have shown that SrFe₂As₂ exhibits structural and magnetic phase transitions at 203 K, where the crystal structure changes abruptly from tetragonal ($I4/mmm$) to orthorhombic ($Fmmm$). Our neutron-scattering experiments confirm the findings of the x-ray measurements for the structural transition while we are able to determine conclusively that the Fe spins in SrFe₂As₂ order antiferromagnetically along the orthorhombic a axis and ferromagnetically along the b axis, with the moment direction along the a axis [Figs. 1(a) and 1(b)]. These measurements, together with the recent observation of static long-range AFM order of the Fe sublattice in PrFeAsO (Refs. 19 and 20),

suggest that the collinear AFM order shown in Fig. 1(b) is ubiquitous for the parent compounds of the FeAs-based superconductors.

We use neutron diffraction to study the structural and magnetic phase transitions in crystals grown using the method described in Ref. 21. Our experiments were carried

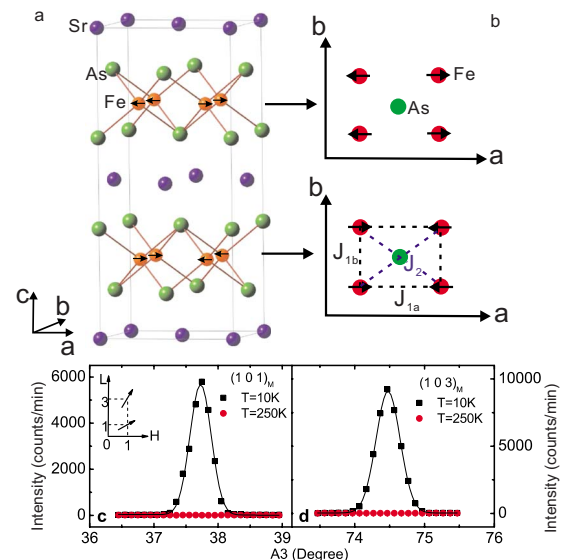


FIG. 1. (Color online) Crystal and magnetic structures of SrFe₂As₂. (a) The three-dimensional AFM structure of Fe in SrFe₂As₂ as determined from our neutron-diffraction data. (b) The in-plane magnetic structure of Fe in the orthorhombic unit cell of SrFe₂As₂. The Fe moments are along the a axis, and form an AFM collinear structure along the a -axis direction and ferromagnetic along the b -axis direction. The nearest-neighbor Fe spins along the c axis are antiparallel, identical to that of LaFeAsO (Ref. 9); J_{1a} , J_{1b} , and J_2 indicate the effective exchange couplings. [(c) and (d)] Radial scans through the magnetic (1,0,1) and (1,0,3) magnetic Bragg peaks below and above the Néel temperature, showing clear resolution-limited magnetic peaks.

out on the conventional triple-axis spectrometer BT-9 at the NIST Center for Neutron Research, Gaithersburg, Maryland. The neutron wavelength employed was 2.359 Å using a pyrolytic graphite (PG) monochromator and PG filter to suppress higher-order reflections to achieve a monochromatic incident beam. The collimations were 40′–47′–S–40′–80′. We denote positions in momentum space using $Q = (H, K, L)$ in reciprocal-lattice units (r.l.u.) in which Q (in Å⁻¹) = $(H2\pi/a, K2\pi/b, L2\pi/c)$, where $a = 5.5695(9)$, $b = 5.512(1)$, and $c = 12.298(1)$ Å are lattice parameters in the orthorhombic state at 150 K. The sample ($\sim 5 \times 5 \times 0.5$ mm³, mosaic $\sim 0.3^\circ$) was mounted on an aluminum plate and aligned in the $[H, 0, L]$ zone inside a sealed aluminum container with helium exchange gas, and mounted on the cold finger of a closed cycle helium refrigerator.

Figures 1(a) and 1(b) summarize our experiments, which show the Fe spin arrangements with respect to the orthorhombic low-temperature crystal structure. To obtain integrated magnetic intensities necessary for comparison with magnetic structure factor calculations, we carried out radial ($\theta:2\theta$) as well as rocking (θ) scans for a series of magnetic $(1, 0, L)$ and $(3, 0, L)$ peaks, where $L = 1, 3, 5, \dots$. Figures 1(c) and 1(d) show scans for the $(1, 0, 1)$ and $(1, 0, 3)$ peaks below and above the AFM ordering temperature. Sharp, resolution-limited magnetic peaks are observed at 10 K, and completely disappear at 250 K, consistent with establishment of long-range AFM order. A detailed investigation of the low-temperature magnetic Bragg peaks in the $(H, 0, L)$ zone revealed an ordered magnetic structure of Fe ions consistent with previous results on LaFeAsO (Ref. 9), CeFeAsO (Ref. 11), NdFeAsO (Ref. 12), and BaFe₂As₂ (Ref. 14).

In previous x-ray and neutron-diffraction work on BaFe₂As₂ and SrFe₂As₂, it was found that the structural distortion occurs almost simultaneously with the development of AFM order.^{13,14,16–18} To confirm this in our single crystal of SrFe₂As₂, we carried out neutron-diffraction measurements focusing on the $(2, 2, 0)_T$ nuclear Bragg peak, where T denotes the high-temperature tetragonal phase. As a function of decreasing temperature, the $(2, 2, 0)_T$ peak abruptly splits into the $(4, 0, 0)_O$ and $(0, 4, 0)_O$ Bragg peaks below 220 ± 1 K as shown in Fig. 2. Here the subscript O denotes orthorhombic symmetry, and the observation of both $(4, 0, 0)_O$ and $(0, 4, 0)_O$ peaks indicates that our single crystal has equally populated twin domains in the orthorhombic phase. Figure 2(b) compares the structural phase transition and magnetic order parameter in detail as a function of temperature. It is evident that both structural and magnetic phase transitions occur abruptly, consistent with a first-order phase transition. By normalizing magnetic peaks with nuclear structural peaks using the magnetic structure shown in Figs. 1(a) and 1(b), we estimate that the ground-state ordered iron moment is approximately $0.94(4)\mu_B$ at 10 K, where numbers in parentheses indicate one standard deviation statistical uncertainty and μ_B denotes Bohr magneton.

In previous neutron-diffraction work on powder samples of LaFeAsO (Ref. 9), CeFeAsO (Ref. 11), NdFeAsO (Ref. 12), and BaFe₂As₂ (Ref. 13), it was found that the Fe spins order antiferromagnetically along one axis of the low-temperature orthorhombic structure and ferromagnetically along the other axis. However, the actual AFM and ferro-

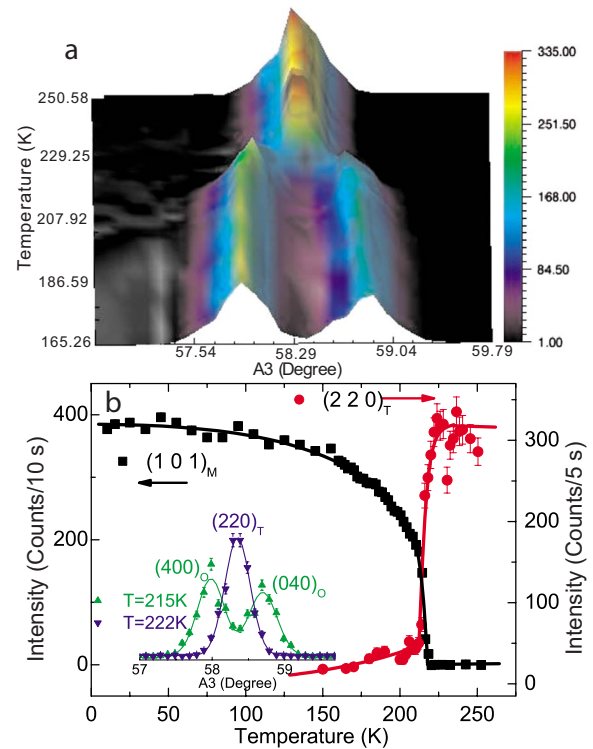


FIG. 2. (Color online) Structural and magnetic phase transition as a function of temperature in single-crystal SrFe₂As₂. (a) Temperature dependence of the $(2, 2, 0)_T$ structural peak, showing that it abruptly splits below 220 ± 1 K. The data were collected using $10' - 11' - S - 10' - 80'$ collimation. (b) Comparison of structural distortion and magnetic order parameter, both occurring at essentially the same temperature. The structural transition is first order, while the magnetic transition appears to be continuous.

magnetic ordering directions, as well as the Fe moment direction, were not determined. To determine the direction of the AFM ordering in SrFe₂As₂, we carefully probed the $(3, 0, 3)$ magnetic Bragg reflection. Figure 3(a) shows a radial scan for the magnetic scattering, where we only observed a single (magnetic) peak. Since the orthorhombic crystal structure of SrFe₂As₂ has twin domains in the $a-b$ plane below the structural distortion temperature, one should observe two separate Bragg peaks along the $[H, 0, 0]$ direction near $(6, 0, 6)$. Removing the PG filter allows both $(6, 0, 6)$ and $(0, 6, 6)$ orthorhombic nuclear Bragg peaks to be observed via $\lambda/2$ in the incident beam at the $(3, 0, 3)$ and $(0, 3, 3)$ positions, respectively. We see that the magnetic peak corresponds to the smaller diffraction angle, which establishes that the AFM ordering is along the a axis. A further check is provided in Fig. 3(b), where the diffraction angle was set to the higher angle reflection, and rocking curves were performed, with and without the PG filter. The only peak observed is the $(0, 6, 6)$ nuclear reflection when the filter was removed. This demonstrates that the only magnetic reflection is the $(3, 0, 3)$ peak. Therefore, our experiments conclusively identify the AFM ordering direction as along the long a -axis direction of the orthorhombic SrFe₂As₂ unit cell.

To determine the Fe moment direction, we carried out integrated intensity measurements for a series of magnetic Bragg reflections. Group symmetry analysis performed in the

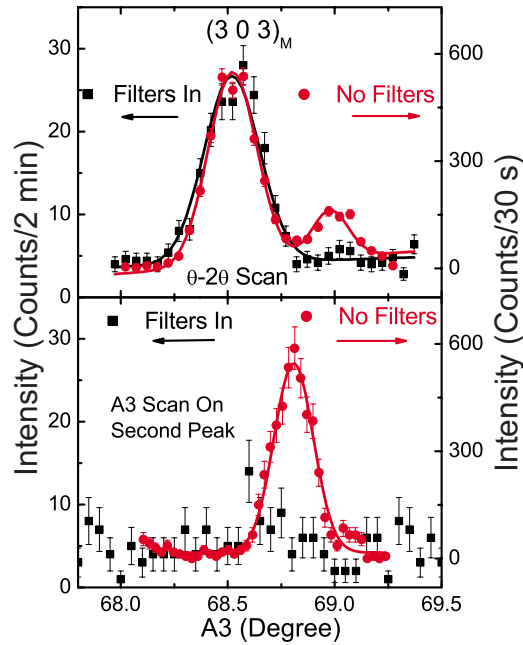


FIG. 3. (Color online) (a) Rocking curves of the (3,0,3) magnetic Bragg peak, and its comparison with structural Bragg peaks obtained from $\lambda/2$ of the nuclear (6,0,6) and (0,6,6) reflections. (b) Identical rocking curve for (0,3,3) magnetic peak position showing no magnetic scattering. This provides definitive evidence that the AFM order occurs along the a -axis direction.

low-temperature $Fm\bar{m}m$ phase restricts the moments to be either along the a , b , or c axis, assuming that the magnetic transition is second order; if it is first order then there are no restrictions on the spin direction. However, if the dominant interactions are determined by Fe-As-Fe exchange, then the orthorhombic structure dictates that the diagonal exchange J_2 in Fig. 1(b) should be the same for both diagonal directions since the bond angles and distances are identical. Therefore we expect the Fe spins in SrFe_2As_2 to point either along the a axis or along the b axis, and this is indeed the case. Assuming the Fe spin direction is ϕ away from the a axis [inset of Fig. 4(a)], the least-squares fit of our magnetic structure factor calculations indicates excellent agreement with a $\chi^2 = 3.8$ for moment along the a axis ($\phi = 4 \pm 3^\circ$). Therefore, it is clear that the moment direction is along a , and the spin structure is shown in Figs. 1(a) and 1(b).

Within the localized magnetism picture,²² the collinear AFM structure can be described in an effective $J_1 - J_2 - J_z$ Heisenberg model,²³⁻²⁵ where J_1 and J_2 are the AFM exchange couplings between the nearest-neighbor and second-nearest-neighbor Fe atoms, respectively, and J_z is the exchange coupling between FeAs layers [Fig. 1(b)]. When $J_1 < 2J_2$, the model has a collinear AFM ground state and also an Ising nematic ordered state at high temperature which can couple to the structural transition in the general Ginzburg-Landau approach. When J_z/J_2 is larger than 0.005, the collinear magnetic and Ising nematic transition temperatures are very close.²⁴ In this model, by including the coupling between the Ising order and the lattice, the structural transition is expected to happen at the same transition temperature as that of the collinear magnetic transition, which provides a

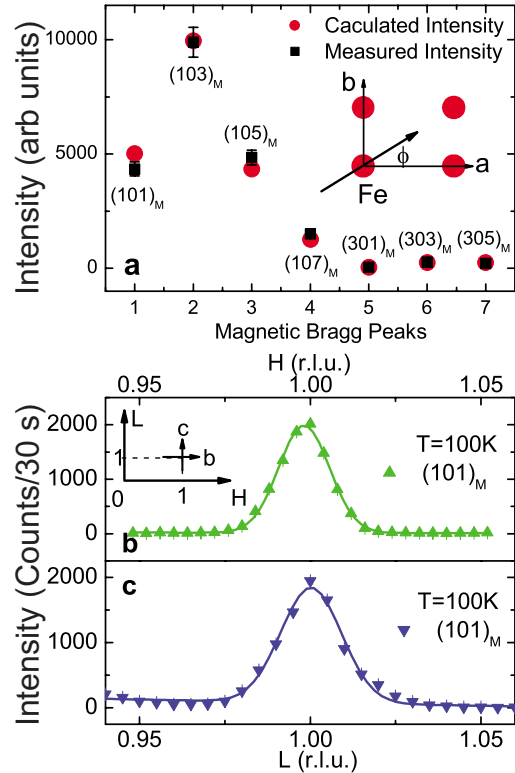


FIG. 4. (Color online) (a) Calculated and observed integrated magnetic Bragg-peak intensities for Fe spin direction along the a axis. The agreement is excellent, demonstrating that the moment direction is along a . ϕ is the angle between Fe spin direction and a axis, which was found to be close to zero for the best fit of the experimental data. [(b) and (c)] Resolution-limited $[H,0,1]$ and $[1,0,L]$ scans through the (1,0,1) magnetic Bragg peak, indicating that the order is long range in nature with a minimum correlation length of 330 Å.

good description for the current case in SrFe_2As_2 , where the interlayer coupling is much larger than that in $R\text{FeAsO}$ compounds.

The observed configuration of orthorhombic lattice distortion and the corresponding spin arrangement reveals that the nearest-neighbor AFM exchange coupling J_1 is not a simple result of a superexchange interaction arising from electron hopping through the As ion since this requires $J_{1a} > J_1 > J_{1b}$ after the lattice distortion in order to save total energy.²³ The fact that the ferromagnetic exchange is along the short (b) axis of the orthorhombic structure suggests the presence of a significant direct ferromagnetic exchange coupling. That is, $J_1 = J_1^s - J_1^d$, where J_1^s is the superexchange AFM contribution and J_1^d is the ferromagnetic part from direct Fe-Fe exchange.

The small lattice distortion has little effect on the local onsite energy but can directly change the electron hopping amplitude. Assume that the high-temperature in-plane tetragonal lattice constant a_T is split into orthorhombic $a = a_T + \delta$ and $b = a_T - \delta$. Then the change of the distance between Fe and the nearest-neighbor As is given by the leading order $\delta^2/4$ [Fig. 1(b)]. Therefore, the change in the hopping amplitude t' after the lattice distortion is $\Delta t' \propto \delta^2$. Since the superexchange $J_1^s \propto t'^4$, its change after the lattice distortion

should be $\Delta J_1^s \propto -\delta^2$. This means that the reduction in J_1^s is a second-order effect of the lattice distortion. On the other hand, since the direct ferromagnetic exchange J_1^d is proportional to the hopping amplitude t , the leading-order changes of J_1^d along the a and b axes after the lattice distortion should be $\Delta J_{1a}^d \propto -\delta$ and $\Delta J_{1b}^d \propto \delta$, respectively. Therefore, J_1 increases along the a axis and decreases along the b axis after the lattice distortion.

In FeAs-based materials, the AFM order is rapidly suppressed upon doping. This immediately suggests a decrease in J_{1a} with increasing doping. Since the decrease in J_{1a} mostly arises from the increase in the direct exchange J_{1a}^d , the long (a) axis of the orthorhombic structure is expected to be suppressed with increasing electron or hole doping. This phenomenon has indeed been observed in electron-doped CeFeAsO and LaFeAsO, where the long (a) axis of the orthorhombic structure is reduced upon doping F while the short (b) axis is unaffected.^{11,26}

In the itinerant magnetism picture,^{27–30} the observed antiferromagnetism in the parent compounds of FeAs-based superconductors has a spin-density wave origin arising from a nested Fermi surface. However, it is unclear why the collinear AFM order should occur along the long a axis of the orthorhombic structure. In summary, we have determined the AFM ordering wave vector and spin direction in SrFe₂As₂, the parent compound of the (Sr, K)Fe₂As₂ superconductors.

Our results indicate that the AFM order shown in Fig. 1(b) is ubiquitous for the parent compounds of FeAs-based superconductors. In addition, to obtain a comprehensive understanding of the mechanism of superconductivity in these FeAs-based superconductors, one must consider both the direct exchange and superexchange interactions, and their relationship to lattice distortion effects.

Note Added: Recently we became aware of a neutron powder diffraction work which also concluded that Fe spins in SrFe₂As₂ order antiferromagnetically in the a -axis direction with ordered moment along the a -axis.³¹

ACKNOWLEDGMENTS

This work is supported by the U.S. National Science Foundation through Contract No. DMR-0756568 and by the U.S. Department of Energy, Division of Materials Science, Basic Energy Sciences through DOE Contract No. DE-FG02-05ER46202. This work is also supported in part by the U.S. Department of Energy, Division of Scientific User Facilities, Basic Energy Sciences. The work at the Institute of Physics, Chinese Academy of Sciences is supported by the National Science Foundation of China, the Chinese Academy of Sciences, and the Ministry of Science and Technology of China.

*daip@ornl.gov

¹P. A. Lee, N. Nagaosa, and X.-G. Wen, *Rev. Mod. Phys.* **78**, 17 (2006).

²Y. Kamihara *et al.*, *J. Am. Chem. Soc.* **130**, 3296 (2008).

³X. H. Chen *et al.*, *Nature (London)* **453**, 761 (2008).

⁴G. F. Chen *et al.*, *Phys. Rev. Lett.* **100**, 247002 (2008).

⁵Zhi-An Ren *et al.*, *Europhys. Lett.* **83**, 17002 (2008).

⁶H. H. Wen *et al.*, *Europhys. Lett.* **82**, 17009 (2008).

⁷M. Rotter, M. Tegel, and D. Johrendt, *Phys. Rev. Lett.* **101**, 107006 (2008).

⁸G. F. Chen *et al.*, *Chin. Phys. Lett.* **25**, 3403 (2008).

⁹C. de la Cruz *et al.*, *Nature (London)* **453**, 899 (2008).

¹⁰M. A. McGuire *et al.*, *Phys. Rev. B* **78**, 094517 (2008).

¹¹Jun Zhao *et al.*, arXiv:0806.2528, *Nature Mater.* (to be published).

¹²Y. Chen *et al.*, *Phys. Rev. B* **78**, 064515 (2008).

¹³M. Rotter *et al.*, *Phys. Rev. B* **78**, 020503(R) (2008).

¹⁴Q. Huang *et al.*, arXiv:0806.2776 (unpublished).

¹⁵K. Sasmal *et al.*, *Phys. Rev. Lett.* **101**, 107007 (2008).

¹⁶C. Krellner *et al.*, *Phys. Rev. B* **78**, 100504(R) (2008).

¹⁷J.-Q. Yan *et al.*, *Phys. Rev. B* **78**, 024516 (2008).

¹⁸Marcus Tegel *et al.*, arXiv:0806.4782 (unpublished).

¹⁹J. Zhao *et al.*, arXiv:0807.4872, *Phys. Rev. B* (to be published 1 October 2008).

²⁰S. A. Kimber *et al.*, arXiv:0807.4441, *Phys. Rev. B* (to be published 1 October 2008).

²¹G. F. Chen *et al.*, arXiv:0806.2648 (unpublished).

²²Q. Si and E. Abrahams, *Phys. Rev. Lett.* **101**, 076401 (2008).

²³T. Yildirim, *Phys. Rev. Lett.* **101**, 057010 (2008).

²⁴C. Fang *et al.*, *Phys. Rev. B* **77**, 224509 (2008).

²⁵C. Xu, M. Müller, and S. Sachdev, *Phys. Rev. B* **78**, 020501(R) (2008).

²⁶Q. Huang *et al.*, *Phys. Rev. B* **78**, 054529 (2008).

²⁷I. I. Mazin *et al.*, *Phys. Rev. Lett.* **101**, 057003 (2008).

²⁸Z. P. Yin *et al.*, *Phys. Rev. Lett.* **101**, 047001 (2008).

²⁹F. J. Ma and Z.-Y. Lu, *Phys. Rev. B* **78**, 033111 (2008).

³⁰J. Dong *et al.*, *Europhys. Lett.* **83**, 27006 (2008).

³¹A. Jesche *et al.*, arXiv:0807.0632 (unpublished).